

## Possibilities of Cirrus Particle Sizing From Dual-Frequency Radar Measurements

S. Y. MATROSOV

*Cooperative Institute for Research in Environmental Sciences, University of Colorado, NOAA, Boulder, Colorado*

This paper considers possibilities of estimating the sizes of ice particles in cirrus clouds using measurements at two radar millimeter wavelengths. The radar frequencies considered are those at the transparency “windows”: 35, 94, 140, and 215 GHz. It is shown that measurements of reflectivity differences at 35 and 215 GHz and at 94 and 215 GHz could potentially be used to estimate particle median sizes from about 0.2 to 0.4 mm. However, the sensitivity of reflectivity differences to particle shapes and orientations will keep the expected error of such an estimation at not less than about 0.1 mm. Measurements of differences in circular depolarization ratios at 35 and 94 GHz, 35 and 215 GHz, 94 and 215 GHz, and 35 and 140 GHz can also be used to estimate particle sizes, and the combination of 35 and 215 GHz can lower the limit of estimated median sizes to about 0.1 mm. It is also shown in the paper that an equal volume sphere approach, being a reasonable approximation for describing backscatter by small ice nonspherical particles, gives larger errors when describing backscatter by larger non-Rayleigh particles. Backscatter by these bigger particles shows significant dependence on particle orientation, which results in relatively large errors of sizing.

### 1. INTRODUCTION

Significant attention is now being paid to theoretical and experimental studies of high-altitude cirrus clouds because of the importance of these clouds in the Earth radiation budget and hence their influence on weather and climate components [Stephens *et al.*, 1990]. Two of the most important parameters of cirrus cloud microphysics that determine not only the magnitude but also the sign of cloud feedback on the climatic system, are particle characteristic size and ice water path (IWP), which is defined as vertically integrated ice mass content (IMC). Different combinations of values of IWP and particle characteristic size can result either in a positive or in a negative cloud feedback in climate models [Ebert and Curry, 1992]. Another combination of radiatively important parameters is particle size and concentration because knowing these two and cloud boundaries one can estimate a value of IWP.

The importance of cloud microstructure in climate modeling dictates the demand for efficient remote sensing techniques to estimate microstructure parameters. The most commonly used tools for remote sensing of cirrus clouds are lidars and infrared (IR) radiometers [Platt, 1979, Sassen *et al.*, 1990]. These types of instruments were successfully used for cirrus studies in the extensive multiagency field program FIRE-I, held in October 1986 in Wisconsin [Starr and Wylie, 1990]. The second phase FIRE-II held in November–December 1991 in Kansas also included millimeter wavelength radars in addition to the broad variety of lidars and radiometers [NASA, 1991].

During FIRE-II, NOAA 8-mm wavelength (35 GHz) and Pennsylvania State University 3-mm wavelength (94 GHz) radars demonstrated their capability of measuring weak backscatter echoes from cirrus clouds. In some aspects, radars have an advantage over lidars because the attenuation and multiple scattering of their signals in ice clouds are very small.

Copyright 1993 by the American Geophysical Union.

Paper number 93JD02335.  
0148-0227/93/93JD-02335\$05.00

We note that no remote sensor operating at one wavelength, in principle, can alone yield parameters of interest without a priori information about cloud microstructure or the aid of other sensors. For example, lidar and radar backscattering depends on both particle sizes and concentrations, and different combinations of these parameters can give the same backscattering. IR radiometers can provide information on the integrated optical thickness of clouds  $\tau$ , but there is no unique correspondence between  $\tau$  and integrated ice water content (IWC) because this relationship depends on the characteristic size of particles [Matrosov *et al.*, 1992]. It should be mentioned that there are a number of empirical relationships between cloud characteristics and quantities measurable by one remote sensor. A review of the relationships between IWC and radar reflectivity is given by Sassen [1987]. These relationships, however, are statistical in nature and thus can work well for some experimental situations, but for others they can give significant deviations from results obtained by more accurate techniques [Uttal *et al.*, 1992].

Information on cirrus cloud microstructure can be obtained from combined measurements using different remote sensors or from measurements by one remote sensor at different wavelengths. We mention here recently suggested techniques such as estimation of particle effective sizes and concentrations from IR radiometer and radar measurements [Matrosov *et al.*, 1992], and estimation of particle sizes from spectrometer and radar measurements [Palmer *et al.*, 1993] and from combined lidar/radar measurements [Intrieri *et al.*, 1991].

The lidar/radar technique is based on the dependence of the backscattering ratio at microwave and infrared frequencies on the particle effective size. Because of the large frequency separation, this technique has several difficulties. Lidar and radar often see cloud boundaries differently, and lidar signals are sometimes subject to significant attenuation in ice particle media. This paper concentrates on the possibility of using dual wavelength radar measurements for sizing cirrus particles.

Cirrus clouds usually produce relatively low reflectivities

(generally less than 0 dBZ), and more sensitive millimeter-wavelength radars have advantages over conventional centimeter-wavelength radars in sensing such clouds. To gain size-dependent information from the backscattering ratio, at least one of the radar wavelengths should be beyond the Rayleigh scattering regime for cirrus particles. In addition to the combination of radar frequencies that was available in FIRE-II (35 and 94 GHz), we also consider combinations of 35 and 215 GHz and of 94 and 215 GHz because of the existence and use of 215-GHz radars for cloud research at short ranges [Mead *et al.*, 1989]. These combinations could be used for aircraft-based radars. Note that the 35-, 94-, and 215-GHz frequencies are located in the middle of atmospheric transparency "windows" in the millimeter-wavelength region, and the use of other frequencies in this region significantly different from those three is not plausible for cloud research (with an exception of the fourth "window" at about 130–140 GHz) because of the very high attenuation rate in the atmospheric water vapor and oxygen. We also consider the combination of 35 and 140 GHz for completeness.

This paper investigates reflectivity and depolarization differences at above mentioned frequencies and analyses potentials for obtaining particle size information from measurements of these differences.

## 2. PARTICLE AND COMPUTATIONAL MODELS

Ice particles in cirrus clouds have many different shapes [Pruppacher and Klett, 1978]. Often, besides the single column, bullet, and plate types of particles, cirrus clouds contain aggregates of irregular shapes [Kosarev and Mazin, 1989]. A lack of adequate information on the aggregate shapes makes modeling of real cirrus particles difficult. The simplest geometrical models that allow the description of polarization properties of backscattering are oblate and prolate spheroids with different minor-to-major aspect ratios. This type of model was successfully used to describe propagation and backscattering of microwaves in different liquid and ice hydrometeors [Oguchi, 1983].

In more recent works concerning radar backscatter [Evans and Vivekanandan, 1990; Aydin *et al.*, 1992], ice crystals were also modeled as hexagonal plates, columns, and needles. Dungey and Bohren [1993] compared the backscattering data calculated using these more realistic shapes with results obtained using spheroidal model with corresponding aspect ratios. The comparisons showed that scattering properties of ice crystals with small size parameters  $x$  ( $x = \pi D/\lambda$ , where  $D$  is the equal volume sphere diameter, and  $\lambda$  is the wavelength) depend largely on the overall shape (i.e., minor-to-major aspect ratio) and not on the subtle differences in specific geometrical cross section shapes. This result coincides with our findings. Usually, data obtained using hexagonal and spheroidal models differ by less than 8–10%.

The aforementioned conclusion shows the suitability of assuming shapes close to spheroidal for the purpose of this work. Takano *et al.* [1992] suggest using the spheroidal model for size parameters up to 30, which is much greater than the largest size parameter considered in this work. We also assume that the aggregate shapes can be modeled by spheroidal (or close to spheroidal) shapes with the aspect ratio estimated from two-dimensional particle images in

direct probes. This assumption is reasonable because there is no comprehensive studies of irregular ice particle shapes which can allow mathematical modeling of shape.

Calculating the backscattering properties of spheroidal particles that are much smaller than the radiation wavelength (in the Rayleigh regime) is relatively easy [Bohren and Huffman, 1983; Van de Hulst, 1983]. Calculations in the resonance regime when particles are neither small nor large compared with the wavelength is more difficult; here we use the perturbative approach developed by Morrison and Cross [1974] for computations of forward scattering amplitudes of large nonspherical rain drops. This approach was also used for calculating radar reflectivities and depolarization ratios of hydrometeors [Matrosov and Timofeyev, 1988].

One shape of an axisymmetric particle is described by

$$P(\omega) = D(b)[0.5 + \zeta(0.25 \sin^2 \omega - 1/6)], \quad (1)$$

where  $P(\omega)$  is the radius vector from the center of the particle to its surface at the angle  $\omega$  from the symmetry axis, and  $D$  is the diameter of the equal volume sphere. The parameter  $b$  is the particle's aspect ratio which can be expressed in terms of  $\zeta$ :

$$b = (1 - \zeta/3)/(1 + \zeta/6) \text{ for oblate particles } (\zeta > 0) \quad (2)$$

$$b = (1 + \zeta/6)/(1 - \zeta/3) \text{ for prolate particles } (\zeta < 0) \quad (3)$$

As an illustration, Figure 1 schematically shows the prolate and oblate shapes with aspect ratios  $b$  of 0.8 and 0.5 obtained by rotation of the cross section given by (1) along the vertical axis.

Measurable radar parameters can be expressed in terms of particle backscattering amplitudes. The solutions for complex backscattering amplitudes are expanded in series with respect to the parameter  $\zeta$ . For relatively small values of  $\zeta$  ( $|\zeta| \leq 0.6$ ), first-order approximation with respect to  $\zeta$  gives acceptable results [Morrison and Cross, 1974]. For particles with higher degree of eccentricity, accounting for higher-order terms can be necessary. For  $\zeta = 0$ , the series for scattering amplitudes reduce to the well-known Mie solutions for spheres.

The perturbative approach can be used for particles with minor-to-major aspect ratios  $b \geq 0.5$ . Accounting for higher-order terms could be, however, required. Using this approach for particles with a smaller aspect ratio makes the calculations very laborious, and convergence problems arise. However, most of the circular depolarization ratios (CDR) of cirrus clouds measured with the NOAA 8-mm radar during FIRE-II were below  $-13$  dB. These CDR measurements were performed with a vertically pointed antenna and also during range-height indicator scans at different radar elevation angles. The low CDR values obtained with different illumination geometries most likely could be explained by scattering of particles with relatively high aspect ratios ( $b \geq 0.5$ ). This indicates that such "blocky" cirrus particles are rather common.

For aspect ratios  $b$  close to 1, the shape of a particle defined by (1) is practically spheroidal. As  $b$  values diminish, the shapes given by (1) begin to deviate slightly from spheroidal. In general case, (1) describes oblate and prolate bodies. However, as it was discussed before, it is particle volume and aspect ratio which really matters for backscattering properties.

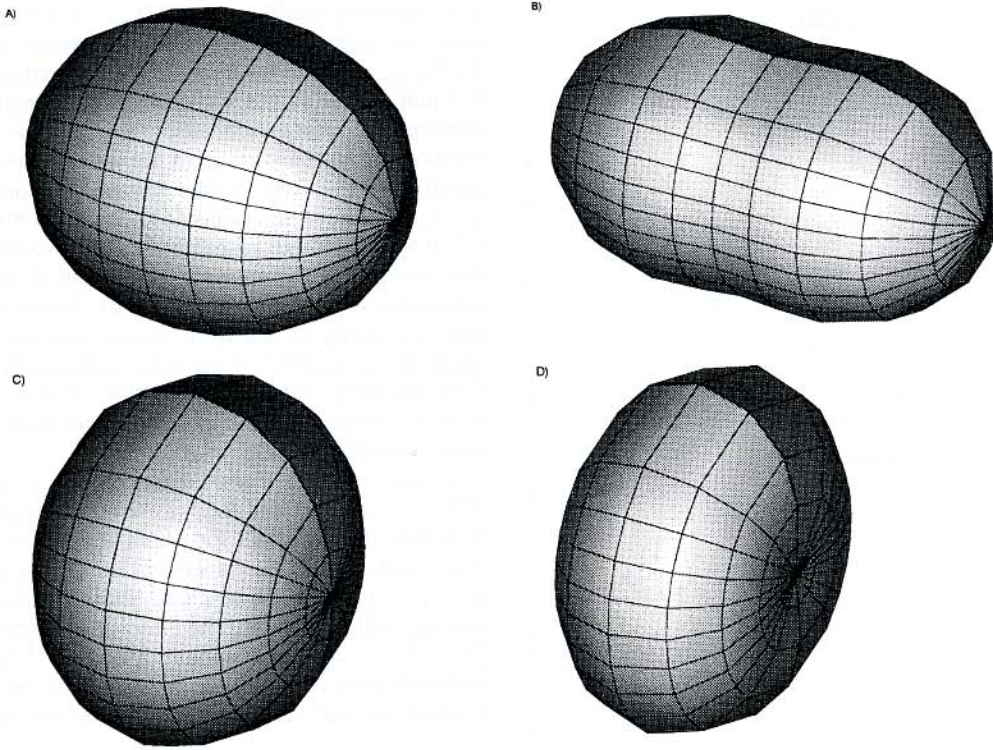


Fig. 1. Schematic shapes of (a) and (b) prolate and (c) and (d) oblate bodies with aspect ratios 0.8 (Figures 1a and 1c) and 0.5 (Figures 1b and 1d).

Modeling of cirrus particle backscattering properties was performed using the model (1) and assuming ice bulk density  $\rho = 0.9 \text{ g cm}^{-3}$ .

### 3. RESULTS OF MODELING

The possibility of sizing cirrus particles using a dual wavelength radar technique is based on the different dependencies of backscattering properties of particles at two frequencies. Modeling backscattering cross sections of individual scatterers showed that at 35 GHz, cirrus particles are mostly in the Rayleigh regime when their reflectivity increases as the linear dimension to the sixth power. The 10% ( $\sim 0.4 \text{ dB}$ ) deviations from the Rayleigh regime begin to appear when the diameter of the equal volume sphere  $D$  exceeds 1 mm. These deviations depend on the particle aspect ratio and orientation; however, they do not, as a rule, exceed about 30% ( $\sim 1 \text{ dB}$ ) for particles with major dimensions less than 2 mm. At 94 and 215 GHz, deviations from the Rayleigh regime become noticeable at about  $D = 0.3$  and 0.15 mm, respectively.

Analysis of cirrus particle size distribution shows that most of the spectra can be described by the gamma function of the first order [Kosarev and Mazin, 1989]:

$$N(D) = N_0 D \exp(-4.67D/D_m), \quad (4)$$

where  $D_m$  is the median size that splits the particle size distribution into two equal-volume parts. Note that for the size distribution (4), the mean size  $\bar{D}$  is less than median size  $D_m$  by factor of 2.3 ( $\bar{D} \approx D_m/2.3$ ). Further calculations of backscattering properties were performed using this distri-

bution function and assuming that the maximum size of cirrus particles is 2 mm.

#### 3.1. Reflectivity Differences

Most meteorological radars use either linear or circular polarizations of transmitted signals. Radar observables on linear polarizations; that is, reflectivities (either vertical  $Z_v$  or horizontal  $Z_h$ ), and linear depolarization ratios (LDR) show significant dependence on particle orientation [Matrosov, 1991]. Circular polarization reflectivities  $Z_c$  and CDR do not depend on the particle canting angle, one of two angles that determine relative geometry of the incident wave and scatterer and hence show less variation due to particle orientation. This makes circular polarization preferable when there is uncertainty about particle orientation. Further analysis will be given in terms of circular polarization radar parameters.

Radar reflectivity and CDR can be expressed in terms of backscattering amplitudes on the horizontal  $S_{hh}$  and vertical  $S_{vv}$  polarizations:

$$Z_c = \frac{1}{4} (\lambda/\pi)^6 |(m^2 + 2)/(m^2 - 1)|^2 \langle |S_{vv} - S_{hh}|^2 \rangle \quad (5)$$

$$\text{CDR} = 10 \log_{10} (\langle |S_{vv} + S_{hh}|^2 \rangle / \langle |S_{vv} - S_{hh}|^2 \rangle), \quad (6)$$

where  $\lambda$  is the wavelength,  $m$  is the complex refractive index of the particle, and the angular brackets mean averaging with respect to size, shape, and orientation distributions. Note that unlike for forward scattering, for backscattering, amplitudes  $S_{vv}$  and  $S_{hh}$  have opposite signs for the optical convention used here.

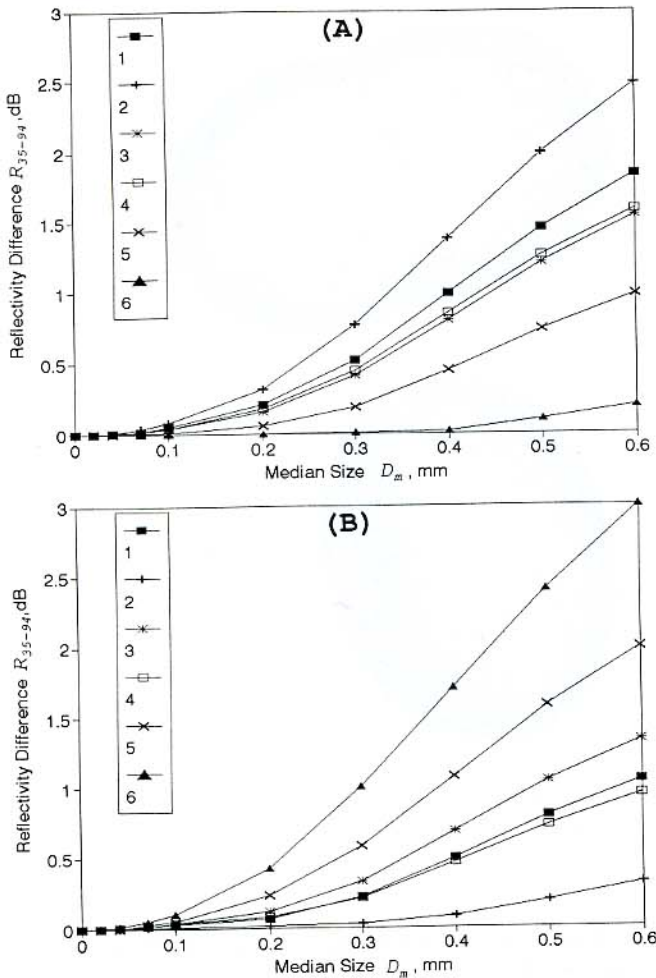


Fig. 2. Differences between radar reflectivities at 35 and 94 GHz  $R_{35-94}$  as a function of (a) oblate and (b) prolate particle median diameter  $D_m$  for different aspect ratios  $b$  and orientation angles  $\alpha$ : 1 -  $b = 0.8$ ,  $\alpha = 90^\circ$ , 2 -  $b = 0.5$ ,  $\alpha = 90^\circ$ , 3 -  $b = 0.8$ ,  $\alpha = 60^\circ$ , 4 -  $b = 0.5$ ,  $\alpha = 60^\circ$ , 5 -  $b = 0.8$ ,  $\alpha = 30^\circ$ , 6 -  $b = 0.5$ , and  $\alpha = 30^\circ$ .

Because of the lack of reliable information about orientation and shape distributions of "blocky" cirrus particles, we performed only size averaging (using (4)) for fixed orientations and shapes. To assess the effects of shape and orientation, calculations were performed for different aspect ratios  $b$  for both oblates and prolates, and for different values of the angle ( $\alpha$ ) between particle symmetry axis and the propagation direction of the incident wave.

Figures 2-5 show the differences between reflectivities of a particle ensemble at 35 and 94 GHz, at 35 and 215 GHz, at 94 and 215 GHz, and at 35 and 140 GHz as a function of the particle median size  $D_m$ . These differences are expressed in decibels and denoted as  $R_{35-94}$ ,  $R_{35-215}$ ,  $R_{94-215}$ , and  $R_{35-140}$  respectively:

$$R_{f-F} = 10 \log_{10} (Z_c(f)/Z_c(F)), \quad (7)$$

where  $f$  and  $F$  are the first and second frequencies in a pair. One can see that all ratios  $R_{f-F}$ , as a rule, increase with the particle median size.

The  $R_{35-94}$  and, to a certain extent,  $R_{35-140}$  differences also depend considerably on particle shape and orientation.

For relatively small particles ( $D_m \leq 0.1$  mm), these differences are negligible. They do not get greater than about 1 dB for  $R_{35-94}$  and 2 dB for  $R_{35-140}$  for larger particles with  $D_m \leq 0.3$  mm. These values are of an order of magnitude for the atmospheric attenuation difference at these frequencies in the layer from the surface to the average height of a cirrus cloud base ( $\sim 8$  km). Under normal meteorological conditions, one-way attenuations at 35, 94, and 140 GHz are about 0.2, 0.9, and 1.8 dB, respectively. We also note that usually the accuracy of the absolute calibration of reflectivity measurements is not better than 0.5 dB. These factors and the high sensitivity of  $R_{35-94}$  to shapes and orientations make sizing cirrus particles using radar reflectivities at 35 and 94 GHz probably not very promising. The 35-140 GHz frequency combination can potentially be used to detect only large particles with  $D_m \geq 0.3$  mm.

As one can see from Figures 3 and 4, the reflectivity differences  $R_{35-215}$  and  $R_{94-215}$  are much greater than  $R_{35-94}$ ; however, they are still too small for  $D_m \leq 0.1$  mm. The shape and orientation dependencies of  $R_{35-215}$  and  $R_{94-215}$  for  $D_m > 0.2$  mm are less than those for  $R_{35-94}$ ; however, they are still significant. The atmospheric attenuation rate at 215 GHz is very high (about  $2 \text{ dB km}^{-1}$  for the normal meteorological conditions), which must be carefully accounted for and limits applications by the studies at close

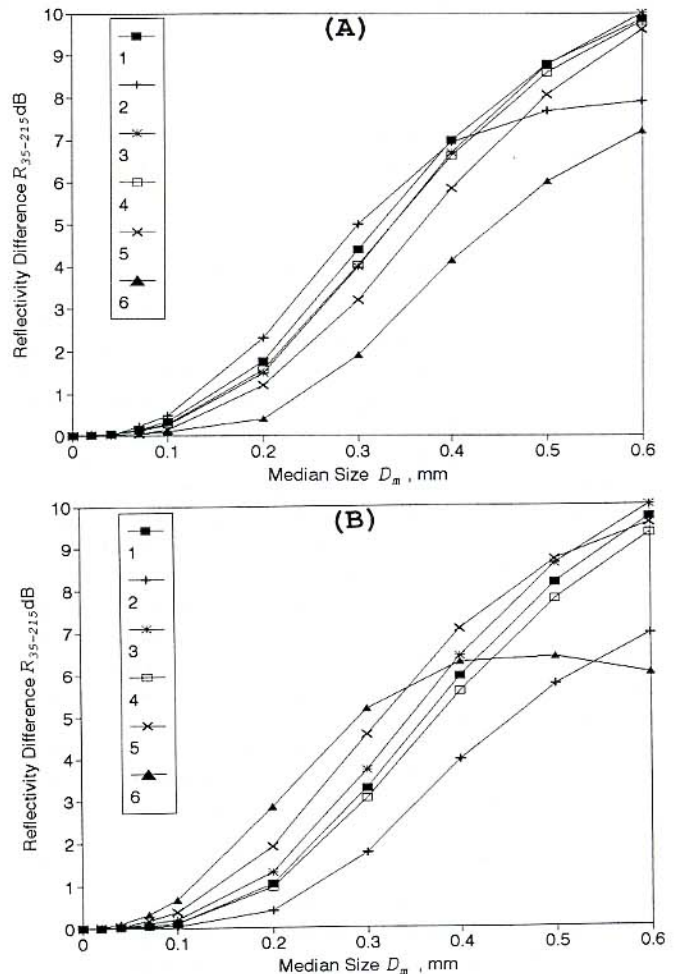


Fig. 3. Same as Figure 2, but for reflectivity differences at 35 and 215 GHz.

ranges. Attenuation and errors in absolute reflectivity calibrations will probably make measurements of  $R_{35-215}$  less than 1–2 dB unreliable. One possibility to reduce the calibration errors is to match the reflectivity data at both frequencies at the cloud top, where one can expect small particles. This heuristic rule will not work, however, with updrafts, which can be identified from Doppler velocity measurements and are not, in any case, common with cirrus clouds.

Measurement error considerations and uncertainty in shape and orientation information suggest that  $R_{35-215}$  and  $R_{94-215}$  measurements could be used for detecting relatively large particles with  $0.2 \text{ mm} \leq D_m \leq 0.4 \text{ mm}$ . The absolute accuracy of such sizing probably cannot be better than about 0.1 mm because of the ambiguity of the  $R$ - $D_m$  relationships due to the spread in particle orientations and shapes. Measuring at radar elevation angles away from zenith reduces some orientation uncertainty because particles tend to be preferably oriented with their major dimensions in the horizontal plane.

To assess the sensitivity of reflectivity differences to size distribution shape, we also performed calculations assuming that particle size spectra are described by the gamma distributions of the zero and second orders. For the same value of  $D_m$ , this distribution differs from the adopted gamma distribution of the first order (4) by its width. The comparison showed that for the median sizes of possible retrieval ( $D_m \sim$

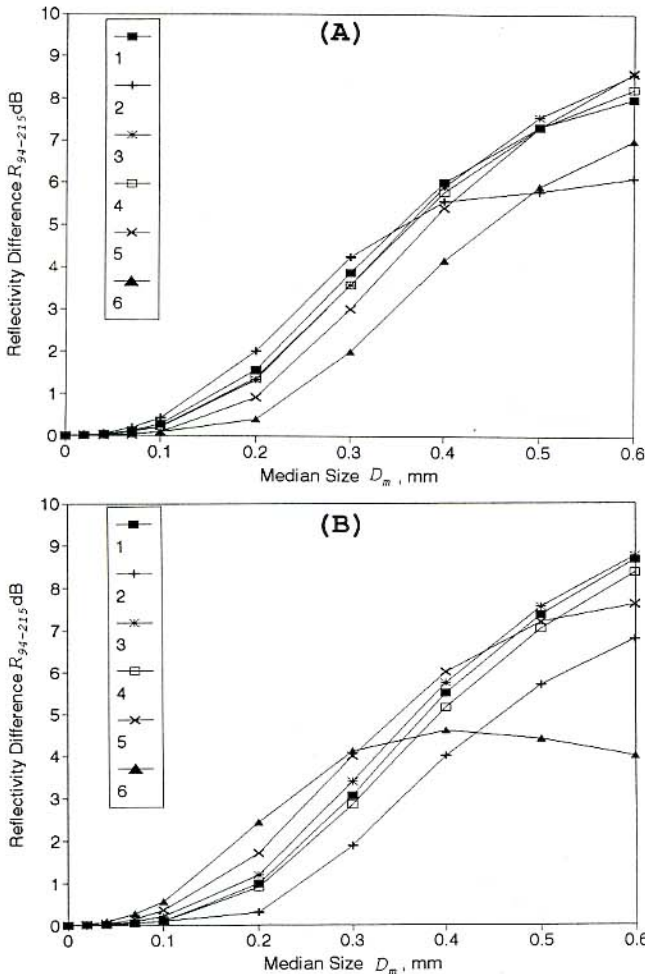


Fig. 4. Same as Figure 2, but for reflectivity differences at 94 and 215 GHz.

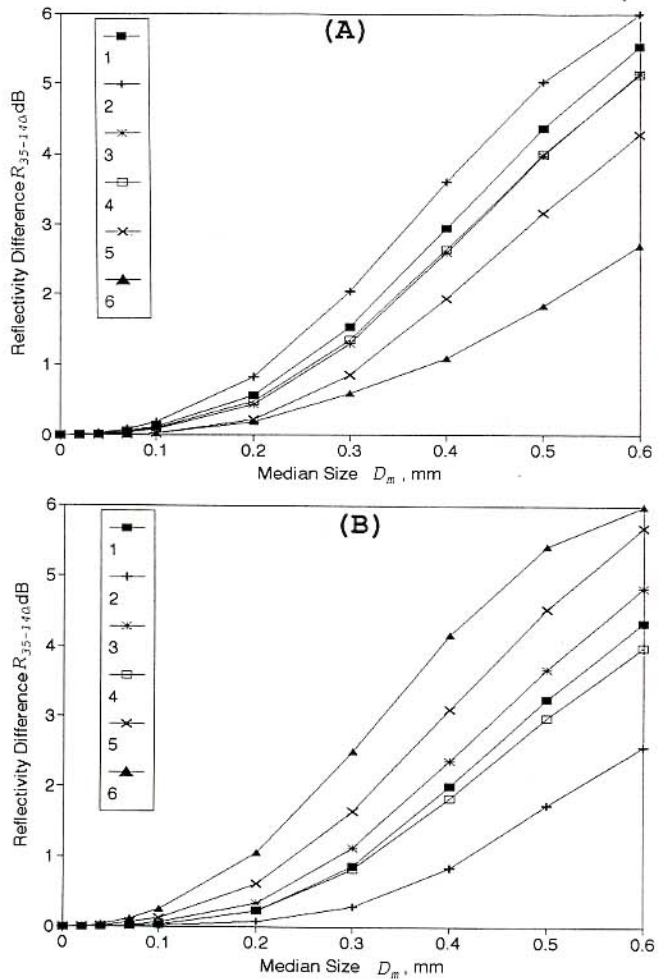


Fig. 5. Same as Figure 2, but for reflectivity differences at 35 and 140 GHz.

0.3 mm), the variations in the size distribution shape translate to variations of  $R_{35-215}$ ,  $R_{94-215}$ ,  $R_{35-94}$ , and  $R_{35-140}$  of 15–20%, which is less than the sensitivity to particle shapes and orientations.

3.2. CDR Differences

Some meteorological radars are capable of measuring reflectivity on two orthogonal polarizations. In case of circularly polarized transmitted radar impulses, the ratio of received echoes on these two orthogonal polarizations represents CDR. CDR values are difficult to measure because of the usually low radar echo on the polarization of the transmitted signals. However, cirrus cloud measurements with the NOAA 35-GHz radar in FIRE-II demonstrated the possibility of measuring CDR from parts of cirrus clouds with relatively high reflectivities.

One advantage of comparisons of CDR at different millimeter wavelengths over comparisons of reflectivities is that the CDR values are not contaminated by atmospheric attenuation because it is cancelled out when taking the power ratio (see equation (6)). In contrast to reflectivity measurements, CDR measurements are also not subject to significant absolute calibration errors.

Figures 6–9 display the differences between CDR of cirrus

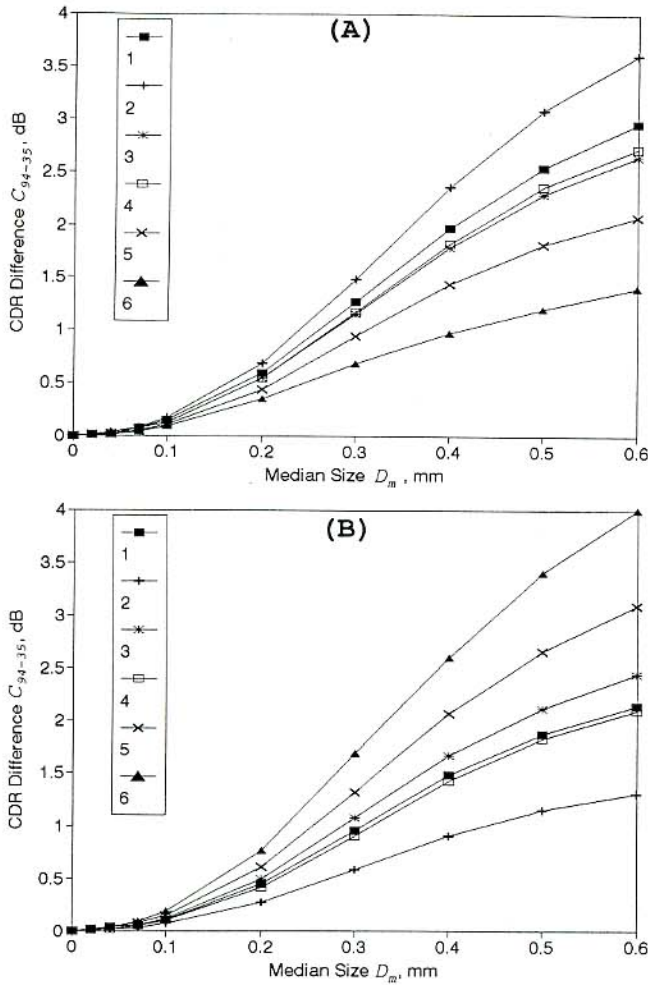


Fig. 6. Differences between CDR at 94 and 35 GHz  $C_{94-35}$  as a function of (a) oblate and (b) prolate particle median diameter  $D_m$  for different aspect ratios  $b$  and orientation angles  $\alpha$ : 1 -  $b = 0.8$ ,  $\alpha = 90^\circ$ , 2 -  $b = 0.5$ ,  $\alpha = 90^\circ$ , 3 -  $b = 0.8$ ,  $\alpha = 60^\circ$ , 4 -  $b = 0.5$ ,  $\alpha = 60^\circ$ , 5 -  $b = 0.8$ ,  $\alpha = 30^\circ$ , 6 -  $b = 0.5$ , and  $\alpha = 30^\circ$ .

particles at 35 and 94 GHz, 35 and 215 GHz, 94 and 215 GHz, and 35 and 140 GHz as a function of the particle median size  $D_m$ . The differences, denoted as  $C_{94-35}$ ,  $C_{215-35}$ ,  $C_{215-94}$ , and  $C_{140-35}$  were calculated for the same particle shapes and orientations as the reflectivity differences:

$$C_{F-f} = CDR(F) - CDR(f) \tag{8}$$

CDR of individual particles increases as the particle size factor  $x$  grows beyond the applicability of the Rayleigh approach. This increase typically continues up to  $x \approx 1.2$  and results in a general increase in CDR differences with an increase of the characteristic size of ice particles.

Although the accuracy of measurements of CDR differences should be higher than that of reflectivity differences, we probably cannot expect errors in  $C_{94-35}$ ,  $C_{215-35}$ ,  $C_{215-94}$ , and  $C_{140-35}$  below about 0.5 dB. As one can see from Figure 6, if radars operating at 35 and 94 GHz are used, this accuracy limit will not allow estimations of cirrus particle sizes for  $D_m \leq 0.2$  mm. Particle ensembles with very high values of  $D_m$  ( $D_m \geq 0.4$ ) can produce significant differences  $C_{94-35}$ ; however, the relatively high sensitivity of  $C_{94-35}$  to particle shapes and orientations and flattening  $C_{94-35}$  versus

$D_m$  dependencies probably will not make accurate particle sizing possible. The only range of  $C_{94-35}$  that could be of any use for estimating particle sizes is probably from about 0.5 dB to about 1.5 dB. These values of CDR differences are produced by cirrus particle ensembles with median sizes from  $\sim 0.2$  to  $\sim 0.4$  mm.

A similar result is probably true for the  $C_{140-35}$  difference. In this case, however, the size region of possible estimates could be about 0.15–0.4 mm. Radar measurements at 35 and 215 GHz and also at 94 and 215 GHz can provide greater CDR differences than those at 35 and 94 GHz. As Figure 7 suggests, values of  $C_{215-35}$  in the range of  $\sim 0.5$  to 4 dB could be used to estimate particle median sizes from  $\sim 0.1$  to 0.4 mm. The accuracy of such estimation cannot be better than  $\sim 0.1$  mm because of the sensitivity of  $C_{215-35}$  to particle shapes and orientations. This error increases with particle size. The combination of 94 and 215 GHz will possibly allow sizing of particles with  $0.1 \text{ mm} \leq D_m \leq 0.3 \text{ mm}$  with the same expected accuracy.

The analysis of sensitivity to size distribution shape showed that the differences between CDR at the examined frequencies are subject to 10–15% variations when the assumed gamma distribution of the first order is changed to the gamma distribution of the zero or second order. These

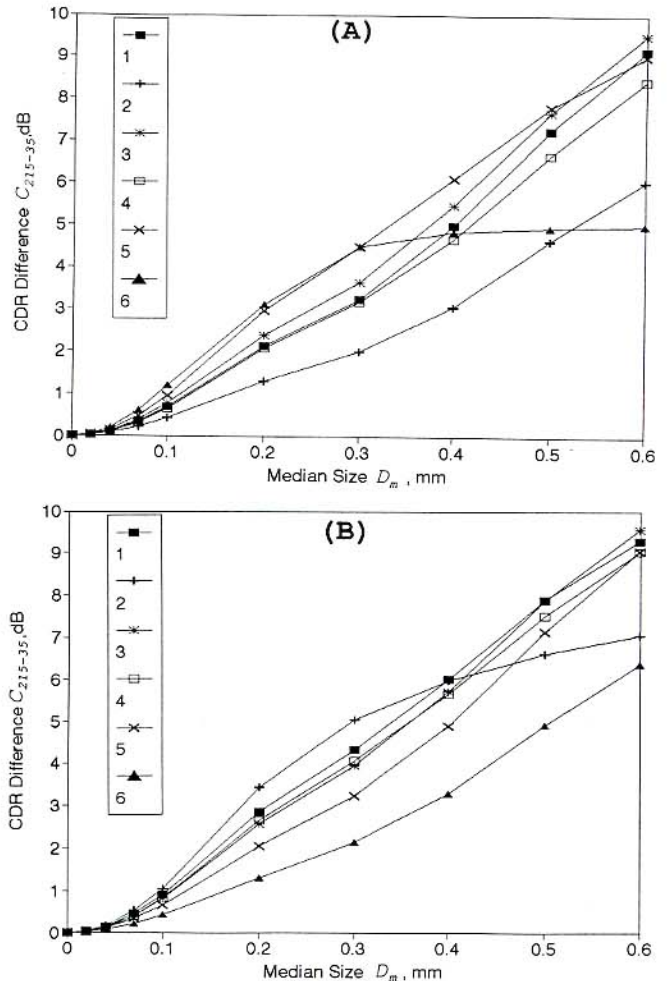


Fig. 7. Same as in Figure 6, but for CDR differences at 215 and 35 GHz.

variations are less than those due to particle shapes and orientations.

As mentioned earlier, CDR measurements in cirrus clouds can be difficult to perform because of the weak signals in one of the radar receivers. In such situations, one possible way to make depolarization measurements possible is to use elliptically polarized radar signals. For elliptical polarizations which are close to the circular polarization, radar echoes in the main receiving channel do not change significantly; however, orthogonal channel echoes increase considerably. This could make possible depolarization measurements of such low reflectivity targets as cirrus clouds [Matrosov and Kropfli, 1993].

### 3.3. Equivalent Sphere Approximation

Modeling atmospheric particles by equivalent spheres is still widely used in many applications, though the spherical model cannot describe some fundamental properties of backscattering such as depolarization. The main reason of using this model is its simplicity. However, for some particular applications, polarization properties are not of interest. One example of such applications is using the empirical relationships between radar reflectivity and IMC [Sassen, 1987]. In

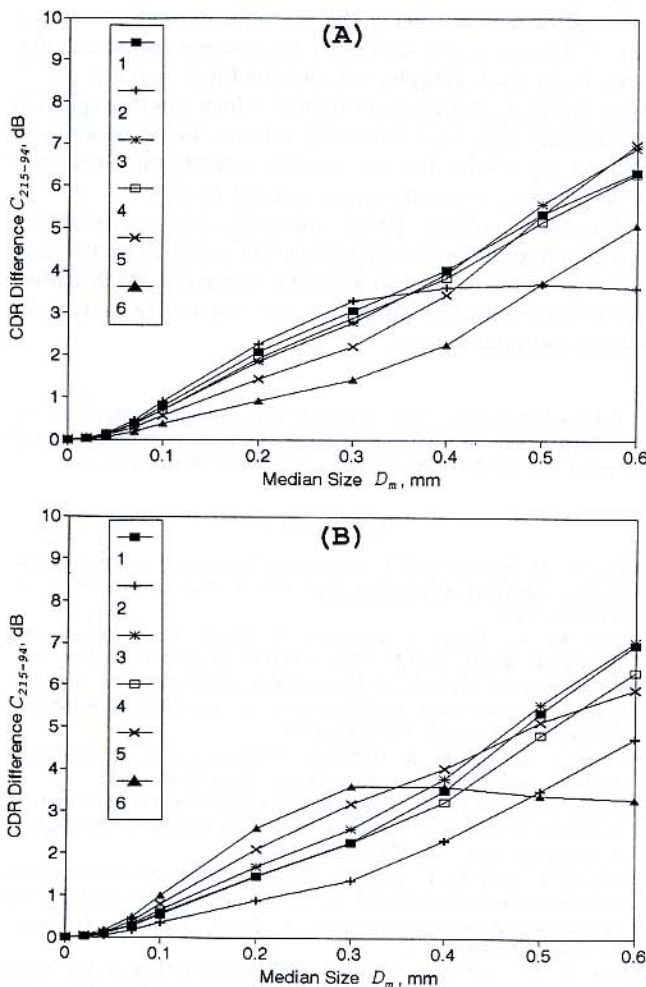


Fig. 8. Same as in Figure 6, but for CDR differences at 215 and 94 GHz.

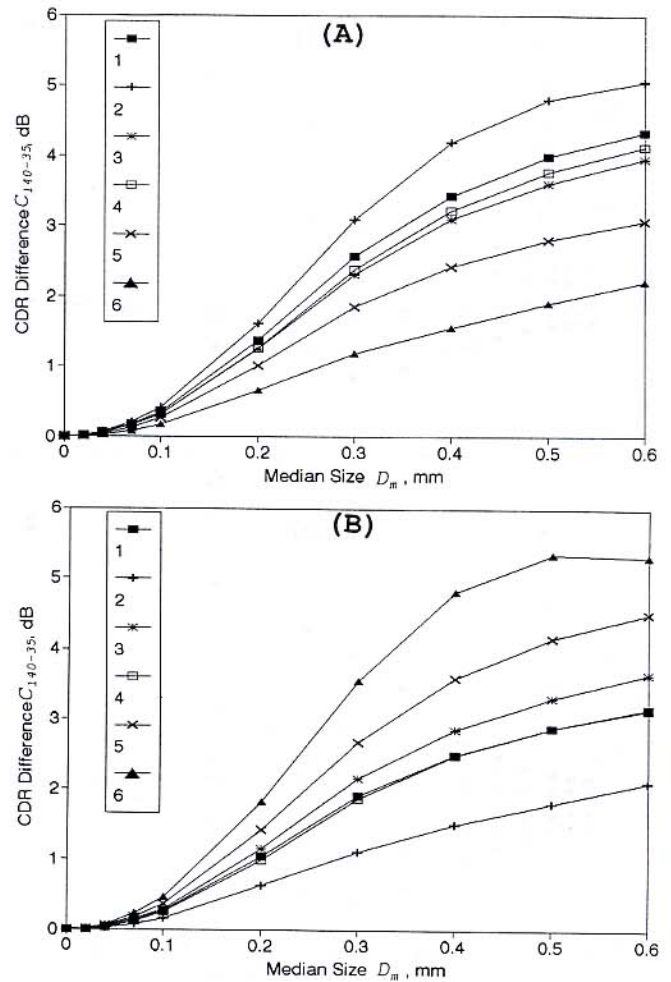


Fig. 9. Same as in Figure 6, but for CDR differences at 35 and 140 GHz.

this case, we need to know the magnitudes of errors when treating nonspherical particles as equivalent spheres.

It was shown by Atlas *et al.* [1953] and Mugnai and Wiscombe, [1980] that equal volume sphere approximation is fairly good for describing backscatter by particles that are small compared with a wavelength. Our calculations show that for small, moderately nonspherical particles with aspect ratios  $b \geq 0.5$ , the differences between circular polarization reflectivities of the nonspherical particles and those of the equal volume spheres do not exceed 1 dB. For spheroidal particles with a higher degree of nonsphericity ( $b \geq 0.2$ ), these differences do not exceed 3 dB. The approximation of the sphere with equal cross-sectional area usually gives worse results [Bohren and Singham, 1991]. The corresponding differences can exceed 1 order of magnitude.

For backscattering of moderately nonspherical aerosol particles that are not small compared to the wavelength, Mugnai and Wiscombe [1980] found that the equal volume approximation becomes worse as the particle size factor  $x$  grows. We performed similar calculations for ensembles of ice particles in the millimeter-wavelength region. Figure 10 shows how  $r$ , the ratio of reflectivity of nonspherical particles to that of the equal volume spheres depends on the size factor  $x_m = \pi D_m / \lambda$ . Calculations were made for the size distribution given by (4).

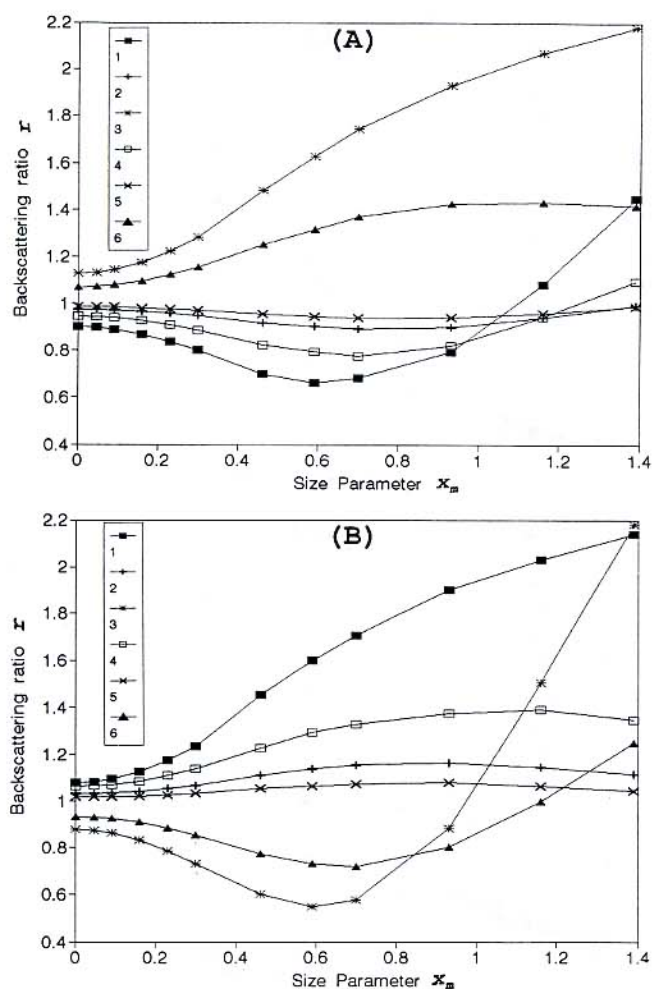


Fig. 10. Ratio of reflectivities of (a) oblate and (b) prolate ice particles to those of equal volume spheres as a function of particle effective size factor  $D_m$  for different aspect ratios  $b$  and orientation angles  $\alpha$ : 1 -  $b = 0.5$ ,  $\alpha = 90^\circ$ , 2 -  $b = 0.5$ ,  $\alpha = 60^\circ$ , 3 -  $b = 0.5$ ,  $\alpha = 30^\circ$ , 4 -  $b = 0.7$ ,  $\alpha = 90^\circ$ , 5 -  $b = 0.7$ ,  $\alpha = 60^\circ$ , 6 -  $b = 0.7$ , and  $\alpha = 30^\circ$ .

It can be seen from data in Figure 10 that the sensitivity of ratio  $r$  to particle shapes and orientations becomes greater as the size factor  $x_m$  increases. This results in the greater ambiguity of the  $R$ - $D_m$  and  $C$ - $D_m$  relationships for big values of  $D_m$ . The equal volume approximation for particles beyond the Rayleigh regime generally becomes worse.

#### 4. CONCLUSIONS

This paper examines the possibility of sizing cirrus cloud particles using radar measurements at two frequencies in the millimeter-wavelength region based on different regimes of scattering at these two frequencies. The combinations of frequencies of existing radars are considered. It is shown that differences of radar reflectivities at 35 GHz and 94 GHz for particle median sizes  $D_m \leq 0.3$  mm are too small to be measured reliably. For larger sizes, uncertainty in particle shapes and orientations greatly increases the error of estimation of  $D_m$  from reflectivity differences at 35 and 94 GHz which makes such kind of measurements not very promising. Measurements at frequency combinations of 35 and 215 GHz or of 94 and 215 GHz produce greater reflectivity

differences compared with 35 and 94 GHz which gives a potential for estimating particle median sizes in the region from  $\sim 0.2$  to  $0.4$  mm. Measurements at these frequencies require careful accounting for the difference in the atmospheric attenuation. The 35–140 GHz frequency combination could help with detection of large particles with  $D_m \geq 0.3$  mm.

Unlike dual-frequency reflectivity measurements, CDR measurements are not subject to the differential attenuation in the atmosphere, which potentially makes measurements of CDR differences more accurate. This creates the possibility of estimating particle median sizes in the range from about 0.2 to 0.4 mm using CDR differences measurements at 35 and 94 GHz. Higher CDR differences at 35 and 215 GHz or at 94 and 215 GHz could lower the limit of possible detection to about 0.1 mm (or 0.15 mm in the event of the 35–140-GHz frequency combination). The sensitivity of CDR differences to particle shapes and orientations keeps an expected error to be greater than about 0.1 mm and does not allow sizing particles with  $D_m \geq 0.4$  mm. This error increases with particle size. Smaller particles, with  $D_m \leq 0.1$  mm, cannot be sized using radar measurements at 2-mm wavelengths because of the close backscatter regimes. Measurements at lower elevation angles are preferable because of reduced orientation uncertainty; however, they are subject to more attenuation.

As mentioned before, the calculations discussed above were performed assuming the ice bulk density  $\rho = 0.9$  g  $\text{cm}^{-3}$ . To assess the sensitivity to  $\rho$ , some model calculations were made (graphs not shown) for  $\rho = 0.6$  g  $\text{cm}^{-3}$ . Main results in this case are similar, which can be explained by the fact that we considered relative radar parameters ( $R_{f-f}$ ,  $C_{f-f}$ , CDR), but not absolute reflectivities. Changes in  $R_{f-f}$  and  $C_{f-f}$  usually do not exceed 15–20%.

The equal volume sphere approach, being a relatively good approximation for reflectivities of small ice particles, is not as good for larger non-Rayleigh scatterers. Backscattering of large particles shows greater sensitivity to particle shapes and orientations.

*Acknowledgments.* This research was funded, in part, by the U.S. Department of Energy's Atmospheric Radiation Measurement Program and the NOAA Climate and Global Change Program.

#### REFERENCES

- Atlas, D., M. Kerker, and W. Hitschfeld, Scattering and attenuation by non-spherical atmospheric particles, *J. Atmos. Terr. Phys.*, **3**, 108–119, 1953.
- Aydin, K., C. Tang, A. Pazmany, J. Mead, R. McIntosh, M. Hervig, R. Kelly, and G. Vali, 94-GHz polarimetric radar scattering from ice crystals, in *Proceedings of the 11th International Conference on Clouds and Precipitation*, pp. 1025–1028, McGill University, Montreal, Canada, 1992.
- Bohren, C. F., and D. R. Huffman, *Absorption and Scattering of Light by Small Particles*, John Wiley, New York, 1983.
- Bohren, C. F., and S. B. Singham, Backscattering by nonspherical particles: A review of methods and Suggested new approaches, *J. Geophys. Res.*, **96**, 5267–5277, 1991.
- Dungey, S., and C. F. Bohren, Backscattering by nonspherical hydrometeors as calculated by the coupled-dipole method: An application in radar meteorology, *J. Atmos. Oceanic Technol.*, **10**, 526–532, 1993.
- Ebert, E. E., and J. A. Curry, A parameterization of ice cloud optical properties for climate models, *J. Geophys. Res.*, **97**, 3831–3836, 1992.
- Evans, K. F., and J. Vivekanandan, Multiparameter radar and

- microwave radiative transfer modeling of nonspherical atmospheric ice particles, *IEEE Trans. Geosci. Remote Sens.*, 28, 423-437, 1990.
- Intrieri, J. M., W. L. Eberhard, and T. Uttal, Determination of cirrus clouds particle effective radii using radar and lidar backscattering data, in *Proceedings of the 25th Conference on Radar Meteorology*, American Meteorological Society, Boston, Mass., 809-812, 1991.
- Kosarev, A. L., and I. P. Mazin, Empirical model of physical structure of the upper level clouds of the middle latitudes, in *Radiation Properties of Cirrus Clouds*, pp. 29-52, Nauka, Moscow, 1989.
- Matrosov, S. Y., Theoretical study of radar polarization parameters obtained from cirrus clouds, *J. Atmos. Sci.*, 48, 1062-1070, 1991.
- Matrosov, S. Y., and R. A. Kropfli, Cirrus cloud studies with elliptically polarized Ka-band radar signals: A suggested approach, *J. Atmos. Oceanic Technol.*, 10, 684-692, 1993.
- Matrosov, S. Y., and Y. M. Timofeyev, Microwave attenuation and scattering characteristics of spheroidal raindrops, *Izv. Akad. Nauk SSSR, Ser. Fiz. Atmos. Okeana*, 24, 808-811, 1988.
- Matrosov, S. Y., T. Uttal, J. B. Snider, and R. A. Kropfli, Estimation of ice cloud parameters from ground-based infrared radiometer and radar measurements, *J. Geophys. Res.*, 97, 11,567-11,574, 1992.
- Mead, J. B., R. E. McIntosh, D. Vandemark, and C. T. Swift, Remote sensing of clouds and fog with a 1.4-mm radar, *J. Atmos. Oceanic Technol.*, 6, 1090-1097, 1989.
- Morrison, J. A., and M. J. Cross, Scattering of a plane electromagnetic wave by axisymmetric raindrops, *Bell Syst. Tech. J.*, 52(4), 955-1019, 1974.
- Mugnai, A., and W. J. Wiscombe, Scattering of radiation by moderately nonspherical particles, *J. Atmos. Sci.*, 37, 1291-1307, 1980.
- NASA, FIRE cirrus intensive field observations, II, Operations plan, in *FIRE Project Office and FIRE Cirrus Working Group*, 116 pp., NASA/Langley Research Center, 1991.
- Oguchi, T., Electromagnetic wave propagation and scattering in rain and other hydrometeors, *Proc. IEEE*, 71, 1029-1078, 1983.
- Palmer, A. J., S. Y. Matrosov, T. Uttal, B. E. Martner, D. K. Lynch, M. A. Chatelain, J. A. Hackwell, and R. W. Russel, Combined infrared emission spectra and radar reflectivity, *IEEE Trans. Geosci. Remote Sens.*, 31, 64-69, 1993.
- Platt, C. M. R., Remote sounding of high clouds, 1, Calculation of visible and infrared optical properties from lidar and radiometer measurements, *J. Appl. Meteorol. Soc.*, 18, 1130-1143, 1979.
- Pruppacher, H. R., and J. D. Klett, *Microphysics of Clouds and Precipitation*, 714 pp., D. Reidel, Norwell, Mass., 1978.
- Sassen, K., Ice cloud content from radar reflectivity, *J. Atmos. Sci.*, 26, 1050-1053, 1987.
- Sassen, K., C. J. Grund, J. D. Spinhirne, M. M. Hardesty, and J. M. Alvarez, The 27-28 October 1986 FIRE IFO cirrus case study: A five lidar overview of cloud structure and evolution, *Mon. Weather Rev.*, 118, 2288-3111, 1990.
- Starr, D. O'C., and Wylie, The 27-28 October 1986 FIRE cirrus case study: Meteorology and clouds, *Mon. Weather Rev.*, 118, 2259-2287, 1990.
- Stephens, G. L., S. C. Tsay, P. W. Stackhouse, Jr., and P. J. Flatau, The relevance of the microphysical and radiative properties of cirrus clouds to climate and climatic feedback, *J. Atmos. Sci.*, 47, 1742-1753, 1990.
- Takano, Y., K. N. Liou, and P. Minnis, The effects of small ice crystals on cirrus infrared radiative properties, *J. Atmos. Sci.*, 49, 1487-1493, 1992.
- Uttal, T., S. Y. Matrosov, J. B. Snider, and R. A. Kropfli, Doppler radar measurements of ice water path and vertical velocities in optically thin clouds: CLARET I and FIRE II results, in *Proceedings of the 11th International Conference on Clouds and Precipitation*, pp. 533-536, McGill University, Montreal, Canada, 1992.
- Van de Hulst, H. C., *Light Scattering by Small Particles*, Dover, New York, 1983.

S. Y. Matrosov, Cooperative Institute for Research in Environmental Sciences, University of Colorado, NOAA R/E/WP6, 325 Broadway, Boulder, CO 80309.

(Received December 17, 1992;  
revised August 6, 1993;  
accepted August 13, 1993.)